SEISMIC DAMAGE OBSERVATIONS OF PRECAST HOLLOW-CORE FLOORS FROM TWO FULL-SCALE SUPER-ASSEMBLY TESTS

Büker, F.[1,*], Parr, M.[2], De Francesco, G.[3], Hogan, L.S.[4], Bull, D.K.[5], Elwood, K.J.[6], Liu, A.[7], Sullivan, T.J.[8]

ABSTRACT

Serious concerns about the life safety risk of hollow-core floors during earthquakes were raised following the collapse of hollow-core units during the 1994 Northridge earthquake and in subsequent laboratory tests. To enhance the understanding of the seismic performance of existing hollow-core floors, a substantial experimental programme of two large-scale super-assembly tests with hollow-core floors was carried out. Each test specimen consisted of a two-bay by one-bay concrete frame with full-scale hollow-core floors, which were constructed using typical 1980s floor detailing. The specimens were loaded with a simulated earthquake record applied quasi-statically.

This paper discusses the progression of hollow-core floor damage observed in both super-assembly experiments. The main findings include the early onset of cracks in the unreinforced webs of the hollow-core units at 0.5% interstorey drift. The tests also demonstrated the detrimental effect of web cracking on the gravity load-carrying capacity of hollow-core floors. Additionally, hollow-core units that are seated at intermediate columns (so-called 'beta units') were found to get damaged more heavily than those supported away from the columns. Moreover, several transverse cracks were observed in the floor soffit away from the support and beyond the provided seating retrofits. Lastly, the extent of floor damage was found to be sensitive to the ground motion, with pulse-type motions (pushing the structure in one direction) tending to cause more severe floor damage than far-field motions with multiple cycles. The paper also outlines key challenges and recommendations for web crack inspections.

1 BACKGROUND

The collapse of precast hollow-core floor units during the 1994 Northridge earthquake raised serious concerns about the seismic resilience of such floors. Subsequent earthquake reconnaissance (Norton et al. 1994) concluded that the failure had initiated at the support connection. This hollow-core floor collapse in the USA raised serious concerns in New Zealand, where hollow-core floors had been widely used since the late 1970s (PCFOG 2009). A series of component tests (Herlihy 1999; Mejia-McMaster 1994; Oliver 1998) furthered the understanding of the seismic performance of hollow-core floor connections, but it was not until the early 2000s that the critical shortcomings of these floors were exposed in a large-scale three-dimensional laboratory experiment (Matthews 2003).

Matthews (2003) tested a segment of a typical precast concrete frame building with hollow-core floors (super-assembly test). As shown in Figure 1, the super-assembly specimen comprised topped 300 mm hollow-core units spanning 12 m over two bays. While the nominal seating of the floors was specified as 50 mm, typical of field conditions, the achieved actual seating length measured 20 mm (east) and 40 mm (west) due to construction tolerances.

PAPER CLASS & TYPE: GENERAL REFEREED

1 PhD Candidate, University of Auckland
2 PhD Candidate, University of Canterbury
3 Research Engineer, University of Canterbury
4 Lecturer, University of Auckland
5 Technical Director, Holmes Consulting
6 Professor, University of Auckland
7 Senior Structural Engineer, BRANZ
8 Professor, University of Canterbury
** frank.bueker@auckland.ac.nz*

(a) Super-assembly specimen with loading rig

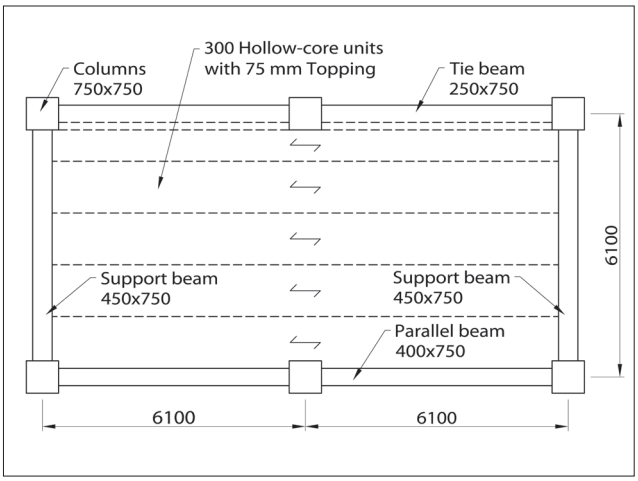

(b) Plan view of the super-assembly specimen

Figure 1: Super-assembly test with 300 mm hollow-core floors (adapted from Matthews (2003))

During Matthews' experiment the hollow-core floors performed in a brittle manner and exhibited critical damage such as:

- A longitudinal tear forming between the first and second unit at 1.9% drift,
- Collapse of the bottom flange of the first unit at 2.0% drift and
- Complete floor collapse after 2.5% drift while loading the floor with design live load.

One of the critical observations was that the damage occurred within the hollow-core units themselves (see Figure 2), disproving previous assumptions that all the deformation and damage manifests at the beam-to-floor interface.

Improved hollow-core floor detailing, which was developed based on the findings from Matthews' test and further testing (Lindsay 2004; MacPherson 2005; Trowsdale 2004), was subsequently introduced into the New Zealand Concrete Structures Standard with the third amendment to NZS3101:1995 (SNZ 2004). These provisions were refined and maintained in NZS3101:2006-A1, A2&A3 (SNZ 2017)). In addition, further investigation into the seismic performance of the pre-2000s hollow-core floor detailing was conducted through several sub-assembly connection tests (Bull and Matthews 2003; Jensen 2006; Liew 2004; Woods 2008). These single hollow-core unit to beam specimens largely contributed to the development of seismic assessment procedures for hollow-core floors published by Fenwick et al. (2010). Three primary modes of failure, namely loss of support (LOS), negative moment failure (NMF) and positive moment failure (PMF), were identified in these assessment procedures.

Hollow-core floor damage found after the 2016 Kaikōura earthquake was of a nature that emphasised the need to

(a) Photo of the support connection after floor collapse

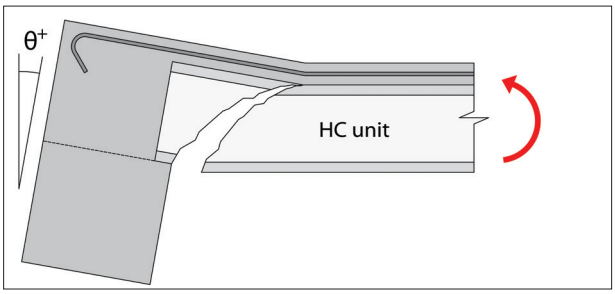

(b) Cross section showing the positive moment cracking generated by relative rotation demands as observed in Matthews' experiment

Figure 2: Cracking within the hollow-core units (adapted from Matthews (2003))

assess and retrofit the many existing pre-2000 hollow-core floor buildings (Henry et al. 2017). The earthquake damage observations and subsequent research (Corney et al. 2018) led to refinements of the seismic assessment methods for precast floors, which were incorporated in the technical proposal to revise Section C5 (Concrete Buildings) of the "Guidelines for Detailed Seismic Assessment of Buildings" (MBIE et al. 2018), from hereon referred to as Assessment Guidelines C5.

Whilst consideration has been given to assessment of the hollow-core floor performance, guidance on hollow-core floor retrofits has been more limited with some options presented in a draft document prepared by the Precast Concrete Floors Overview Group (PCFOG 2009); however, those presented retrofit solutions have remained largely unvalidated.

1.1 RECAST FLOORS PROJECT

The 'ReCast Floors' research project was established with the primary objective of validating existing and developing new precast floor retrofits as well as improving the understanding of the seismic performance of precast floors. As part of the ReCast Floors project, two super-assembly tests were conducted in the laboratory facilities at the University of Canterbury. These tests were primarily carried out to experimentally validate proposed hollow-core floor retrofit solutions but also to address some further questions on the seismic behaviour of existing hollow-core floors, such as:

- What is the seismic performance of a hollow-core floor with common detailing features found in existing pre-2000s buildings? Selected detailing features included:
  - 200 mm hollow-core units spanning a single bay,
  - Units that are seated at intermediate columns (beta β units) and related,
  - Notches in the units to fit the units around columns.
- How does NMF in hollow-core floors progress on a system level?
- At what inter-storey drifts do web cracks form and how do they progress relative to the imposed peak drifts?
- How does floor damage affect the diaphragm performance?

The last of these topics is discussed in detail by Parr et al. (2022a; b).

This paper discusses the floor damage observations from the two ReCast Floors super-assembly tests, addressing the above questions and informing what earthquake damage can be expected in existing hollow-core floor buildings. These damage observations are then compared to demonstrate the effect of different floor detailing and the ground motion sensitivity. The damage observations are further compared to the assessed limiting drifts based on the Assessment Guidelines C5. Lastly, recommendations are made on effective inspection techniques for the detection of web cracks.

2 SUPER-ASSEMBLY SPECIMENS AND SETUP

Two super-assembly specimens were tested in the laboratory facilities at the University of Canterbury, Christchurch, New Zealand. Both test specimens represented a segment of a reinforced concrete frame building with retrofitted hollow-core floors and were each subjected to quasi-static simulated earthquake loading. Whilst the frame components were nominally the same for both test specimens, there were distinct differences in floor detailing, retrofit solutions and loading protocol between the two tests.

2.1 TEST SPECIMENS

The test specimens consisted of two-bay by one-bay reinforced concrete frames with precast hollow-core floor units, as shown in Figure 3. The general frame configuration incorporated typical 1980s Wellington building features, such as the eccentric alignment between beam centreline and column centreline and the resulting protrusion of the columns into the floor plate. The structural design and detailing of the frame components satisfied the latest ductile design provisions in accordance with NZS3101:2006-A3 (SNZ 2017) to ensure that these components had deformation capacity that was sufficient not to influence the experiment. Non-critical parts of the frame structure test specimens (i.e. columns, longitudinal beam reinforcement and the lower middle of the parallel beams) from the first test specimen were re-used for the construction of the second test specimen.

The floor was formed with eight 200 mm deep precast hollow-core floor units spanning 7.1 m in the one-bay direction and a 75 mm deep topping layer reinforced with non-ductile cold-drawn 665 mesh. Each hollow-core floor unit contained five 12.5 mm prestressing strands. The support connections to the frame, shown in Figure 4, replicated 1980s Wellington construction practice. The actual seating length varied for each unit end ranging from 15 to 55 mm.

Four of the eight hollow-core units (U1, U4, U5 and U8 in Figure 3a) were seated on the plastic hinges of the support beams. The hollow-core units U1 and U8, located adjacent to the parallel beams, can be classified as 'alpha (α) units' (Brooke et al. 2022; PCFOG 2009). Previous research has identified that alpha units can be subjected to displacement incompatibilities with the adjacent parallel beam deforming in double curvature while the hollow-core units attempt to remain flat (Fenwick et al. 2010; Matthews 2003; MBIE et al. 2018). Conversely, units U4 and U5 were seated on the plastic hinges at the intermediate columns and classified as 'beta units' (Brooke et al. 2022). The unique boundary conditions of beta units can lead to complex local demands in their support regions. Because previous super-assembly tests (Lindsay 2004; MacPherson 2005; Matthews 2003) did not include beta units, the super-assembly tests described in this paper were designed to gain insights into the seismic behaviour and damage patterns of beta units, particularly when subjected to bi-directional interstorey drift demands, as expected in real buildings.

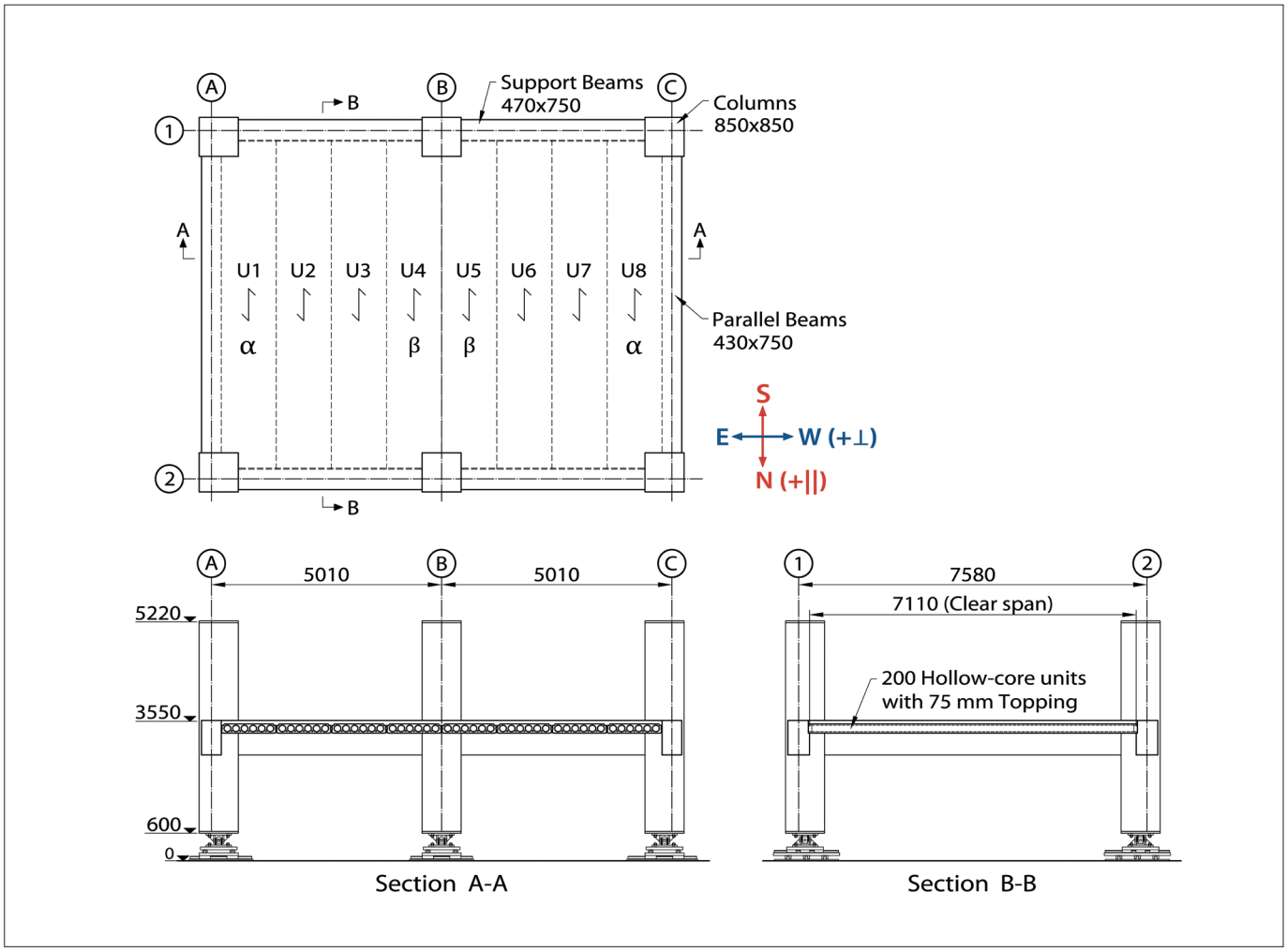

Figure 3: Super-assembly specimen with nominal dimensions.

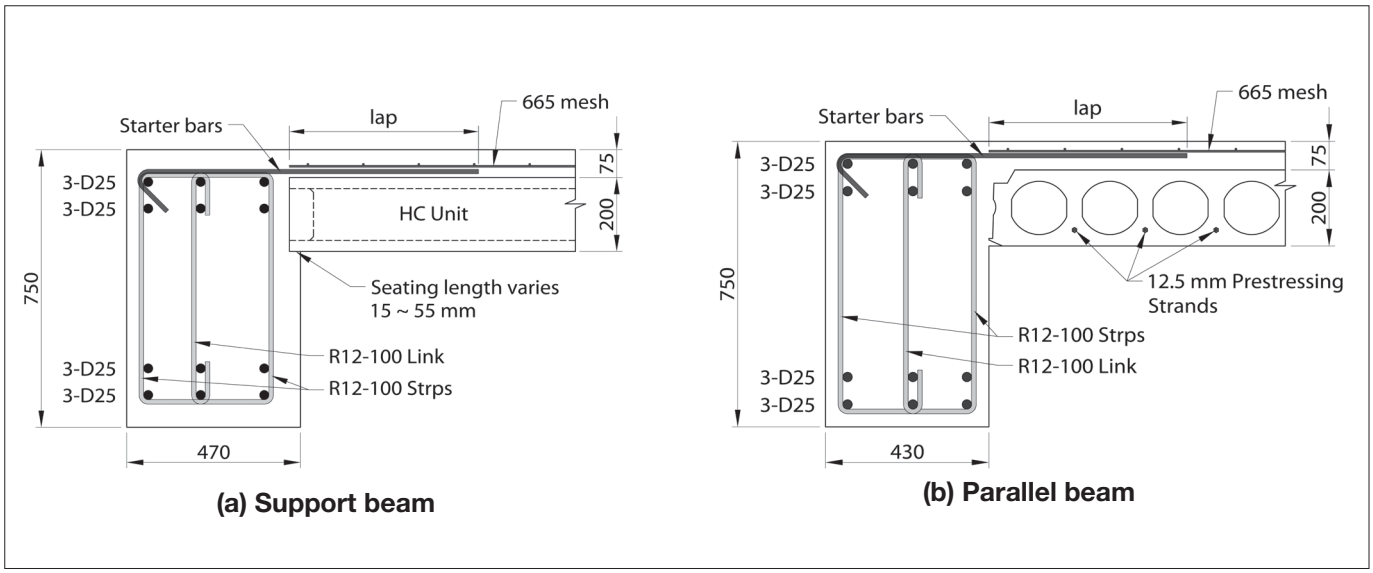

Figure 4: Cross-section view showing the floor-to-beam connections.

2.2 SETUP

The setup for the super-assembly tests, shown in Figure 5, allowed simultaneous bi-directional earthquake loading with 14 actuators installed along an L-shaped strongwall. The actuators were connected to the top and bottom of the columns along the south and east side of the test specimens. Load transfer between the columns was achieved through internal loading frames that acted as pantographs. The bottom of the columns rested on bi-directional sliders with universal hinges. The combination of internal loading frames and sliders ensured that the columns remained parallel while allowing the frame to dilate due to beam elongation. Loading of the test specimens was quasi-static and thus horizontal and vertical accelerations could not be simulated.

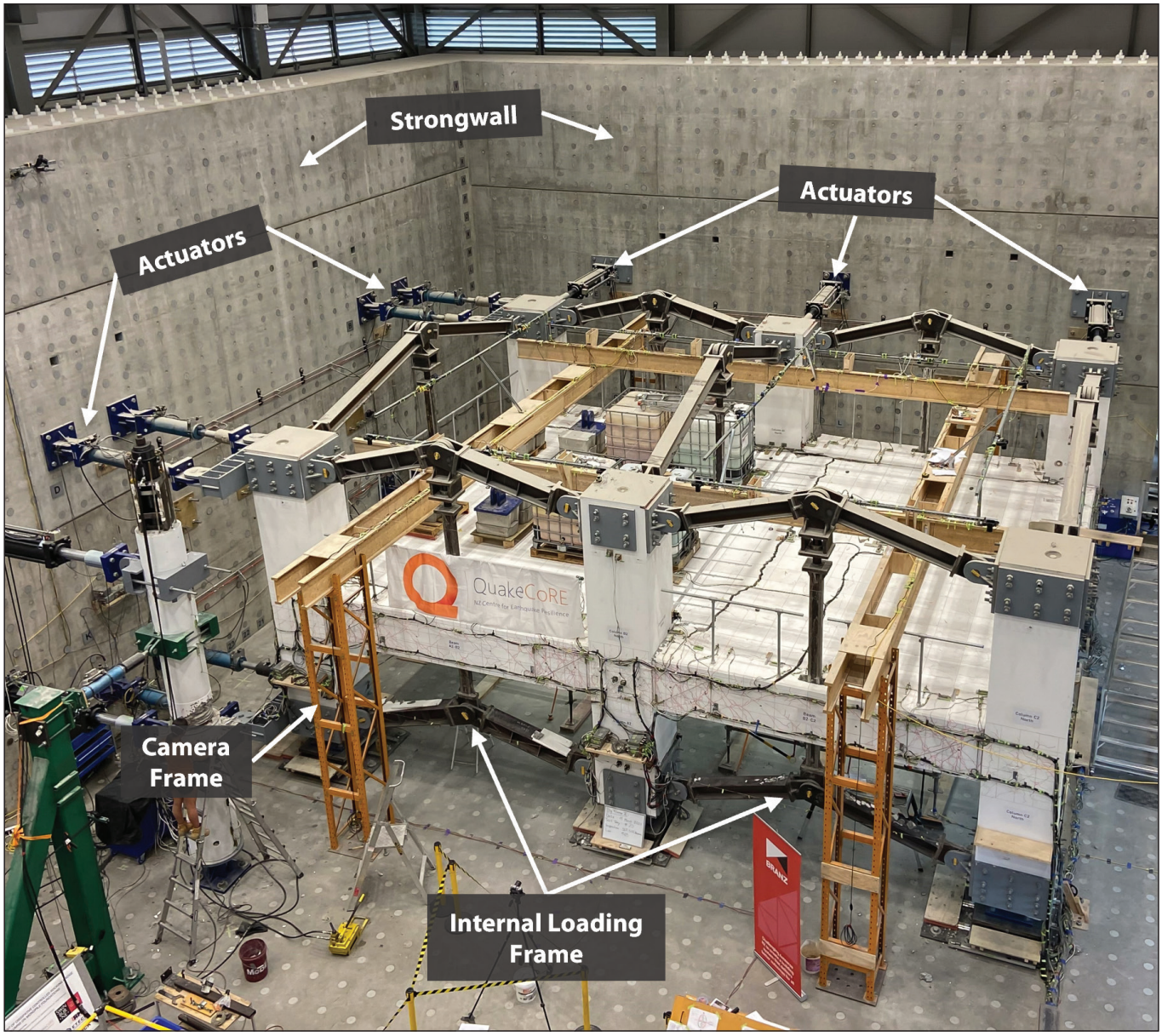

Figure 5: Super-assembly test setup in University of Canterbury laboratory

2.3 TEST CONFIGURATIONS AND LOADING PROTOCOLS

While the frame and setup of the two test specimens were generally similar, there were distinct differences in terms of floor detailing, floor retrofits and loading protocols. These differences are outlined for each of the two tests in Table 1 and elaborated in the following sub-sections. Table 1 also contains references to companion papers with more detail on the retrofits.

Table 1: Summary of floor detailing, retrofits and loading protocols for Tests 1 and 2

	Test 1	Test 2
Starter bar configuration (see Figure 6)	**Beam A1-B1 & A2-B2:** HD12 @400 mm centres with 600 mm lap **Beam B1-C1 & B2-C2:** HD12 @400 mm centres with 600 mm lap and mesh extending into top of the beam	**Beam A1-B1 & B2-C2:** HD12 @400 mm centres with 600 mm lap **Beam B1-C1:** HD12 @300 mm centres with 450 mm lap and mesh extending into top of the beam **Beam A2-B2:** 665 mesh extending into top of the beam (no starter bars)
Retrofits	**Unit U1 & U4:** Catch beams **Unit U2 & U3:** Supplementary seating **Unit U5:** Catch beams + supplementary transverse reinforcement **Unit U6 & U7:** Supplementary seating + supplementary negative moment reinforcement **Unit U8:** Supplementary transverse reinforcement (For conceptual retrofit details, refer to companion paper by Brooke et al. (2022))	**Units U1-U4:** Cable-catch retrofit (Brooke et al. 2022; Büker et al. 2021) **Units U5-U8:** Strongback retrofit (Büker et al. 2022)
Column ties (see Figure 6)	2x HD20 column tie bars (installed prior to casting the topping)	2x HD20 column tie bars (post-installed after casting the topping.) D12 'stitching bars' in transverse direction (reinstating the load path across cut mesh between units U4 and U5.)
Additional gravity weights on floor	No additional loads (only self-weight of the floor)	Additional weights on units U1-U4 in accordance with: $E_d = G + \psi_E Q + E_u$ (SNZ 2011)
Loading protocol (see Figure 7)	**Phase 1:** 2016 Kaikoura Earthquake (far-field) **Phase 2:** Standard Loading Protocol (Bi-directional circular loading pattern)	**Phase 1:** 1994 Northridge Earthquake (pulse-type) **Phase 2:** Standard Loading Protocol (Bi-directional elliptical loading pattern with 1 (‖) to 0.5 (⊥) ratio)

2.3.1 Starter bar configurations

The starter bar configurations at the supports were varied between the two test specimens to investigate the effect of different reinforcement arrangements on the floor performance. For the first specimen, the starter bar configuration was generally kept consistent with slight variations between the two bays (refer to Table 1 and Figure 6a).

Test specimen 2 comprised several different starter bar configurations, as shown in Figure 6b (also refer to Table 1). Most notably, the detailing along B1-C1 was designed to be particularly critical for negative moment failure, firstly to investigate how a negative moment failure evolves on a system level and secondly to test the retrofit solutions for this failure mode. A 30 mm-deep saw cut was made at the end of the starter bars along beam B1-C1 prior to testing to ensure that a negative moment crack formed in this for NMF critical location (Figure 6b). The detailing along beam A2-B2 was in contrast to this highly reinforced connection, with only mesh extending from the topping into the top of the beam. Although the 'mesh only' configuration is not typically encountered along seismic frames, it is more commonly found at internal supports.

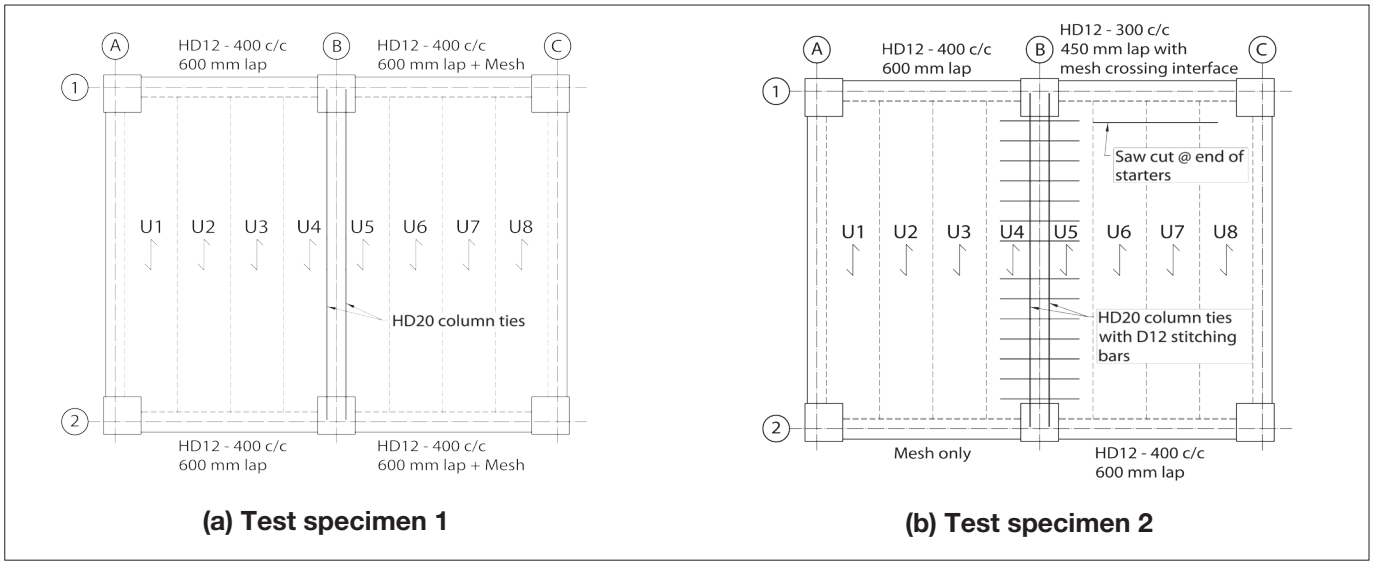

(a) Test specimen 1 **(b) Test specimen 2**

Figure 6: Starter bar configuration and column tie detailing.

2.3.2 Retrofits

Both test specimens comprised a variety of floor retrofits that primarily aimed to prevent the collapse of the flooring units and ensure life safety performance. The retrofits were designed to only actively engage when the floor underwent vertical dislocation relative to the support structure. For this reason, the damage observed at low-to-medium drift levels was not significantly affected by the presence of the floor retrofits. A list of the retrofit solutions that were installed in each test specimen can be found in Table 1. However, it should be noted that this paper does not discuss the performance of the retrofit solutions but only focuses on the floor performance. For more detail on the retrofit solutions refer to the companion papers by Brooke et al. (2022) and Büker et al. (2022).

That notwithstanding, the column tie retrofits, which tie the intermediate columns into the topping layer, warrant further elaboration within this paper because these tie bars actively affected the floor performance. Column tie reinforcement was required for the intermediate columns B1 and B2 as per NZS3101:2006-A3 (SNZ 2017) to prevent the columns from translating outwards. As column ties were typically not installed in existing 1980s precast floor buildings, they were considered a retrofit solution for these tests. For the first test specimen, the column tie bars were epoxied into the inner face of the intermediate columns and placed under the mesh reinforcement before casting the topping concrete. For the second test specimen the column ties were post-installed after the topping concrete had been laid. Grooves were cut into the topping layer, which required cutting the mesh reinforcement to achieve sufficient depth for reinforcement coverage. For this reason 'stitching bars' were needed to be installed across where the mesh had been cut. The grooves for both the column ties and stitching bars were roughened and subsequently filled with high-strength cementitious grout.

2.3.3 Loading Protocols

Two different series of loading protocols were adopted for the two experiments. The loading protocols were developed aiming to represent realistic earthquake loading scenarios for hollow-core floor buildings in Wellington. During the 2016 Kaikōura earthquake a significant number of Wellington buildings incurred damage to hollow-core flooring (Henry et

al. 2017), and consequently the displacement demands in the first test were aimed to simulate shaking from this earthquake. To evaluate the interstorey drift demands imposed by this earthquake, De Francesco and Sullivan (2022) developed a three-dimensional finite element model of a thirteen-storey reinforced-concrete frame building with hollow-core floors featuring typical characteristics of 1980s construction practice in Wellington. Nonlinear time-history analyses were conducted for both horizontal components of the 2016 Kaikōura earthquake record from the CPLB station (Chandramohan et al. 2017). The inter-storey drift response was identified to be largest at the third storey. The response at the third storey was extracted, simplified and converted into a circular bi-directional cloverleaf loading pattern, which is schematically illustrated in Figure 7c. For a clear differentiation of the loading direction, the inter-storey drift demands applied in the direction parallel to the hollow-core unit span (North-South direction) are marked with a '||' symbol and inter-storey drift demands transverse to the unit span (East-West direction) are marked with a '⊥' symbol. After the simulation of the 2016 Kaikōura earthquake, loading was continued with progressively increasing drift levels following the same circular cloverleaf pattern. The entire loading sequence for Test 1 is shown in Figure 7a and is listed numerically in Table 2.

The experimental observations during Test 1 (refer to Section 3.1) highlighted that torsional softening of the frame structure, due to the many bi-directional cycles of the far-field 2016 Kaikōura earthquake motion, can significantly decrease the floor demands. To contrast these findings, the second test simulated a near-fault, pulse-type motion from the 1994 Northridge earthquake recorded at the Rinaldi Receiving Station. The inter-storey drift response was derived using the same procedure as for Test 1. The derived simplified earthquake demand consisted of an initial pulse to -2.0% (||) inter-storey drift, followed by loading to +1.0% (||) and ±1.0% (⊥) as shown in Figure 7b. The directionality from the 1994 Northridge earthquake motion was further continued in the standard loading protocol phase by using an elliptically shaped cloverleaf loading pattern (Figure 7d). The aspect ratio between the parallel (||) and transverse (⊥) direction was 1:0.5. The entire loading sequence for Test 2 is shown in Figure 7b and is listed numerically in Table 3.

Figure 7: Loading protocols with low-intensity cycles to 0.125% drift omitted for clarity. (Note: ROM# refers to the application of Rhomboid loading as shown in Figure 8.)

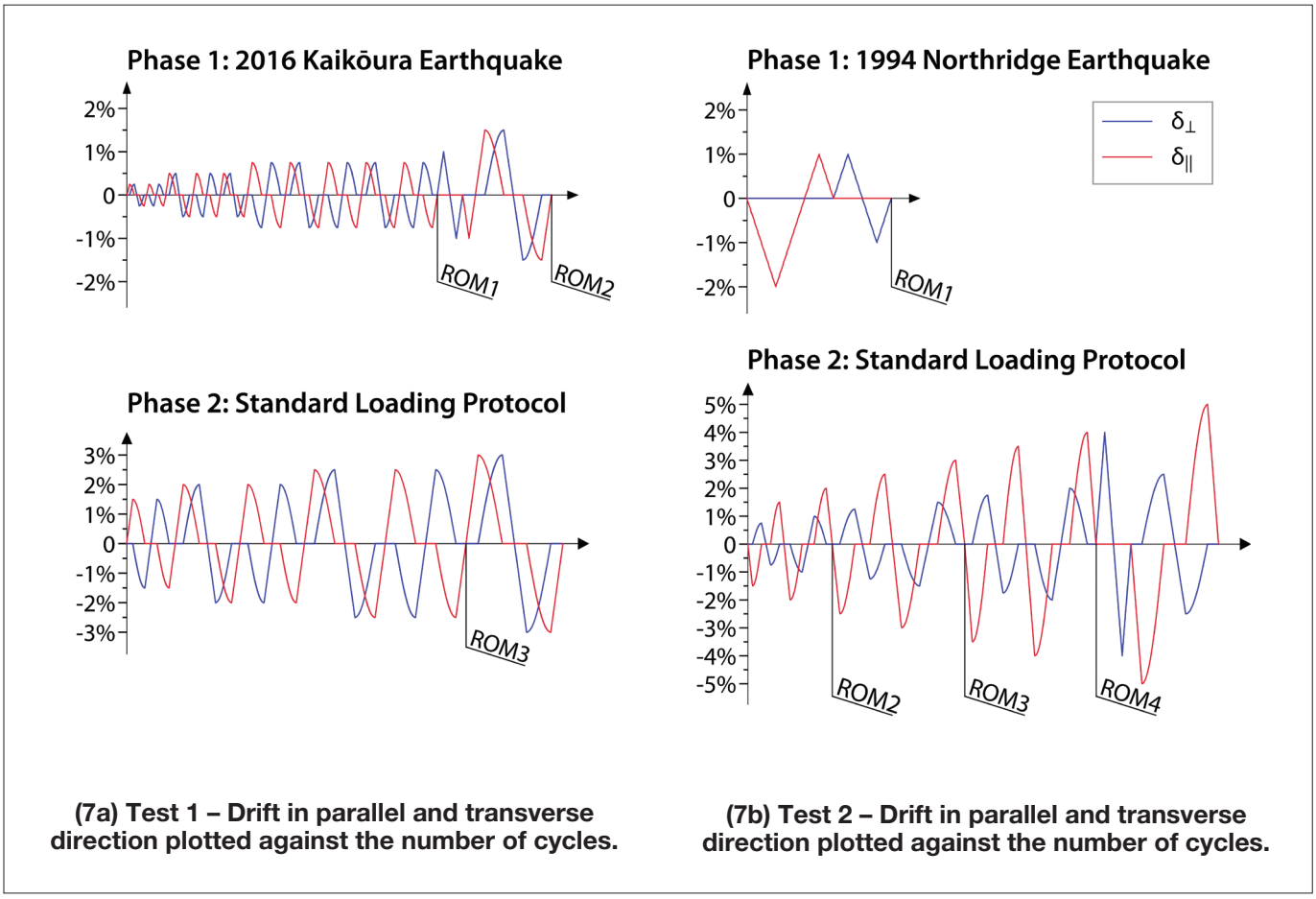

(7a) Test 1 – Drift in parallel and transverse direction plotted against the number of cycles.

(7b) Test 2 – Drift in parallel and transverse direction plotted against the number of cycles.

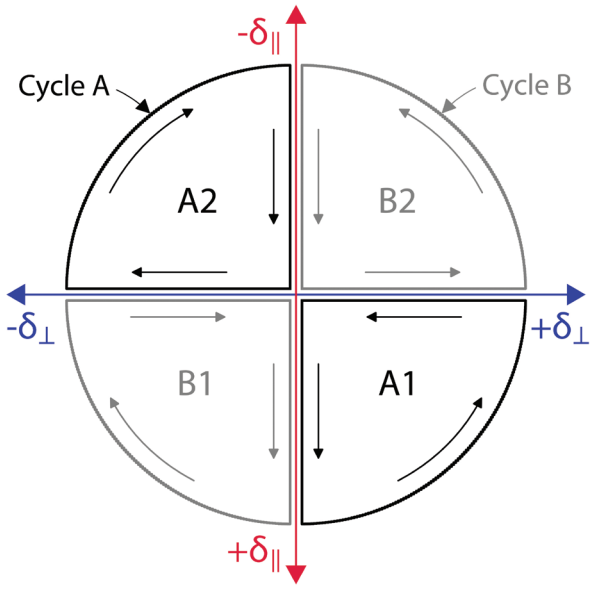

(7c) Test 1 – Circular loading pattern

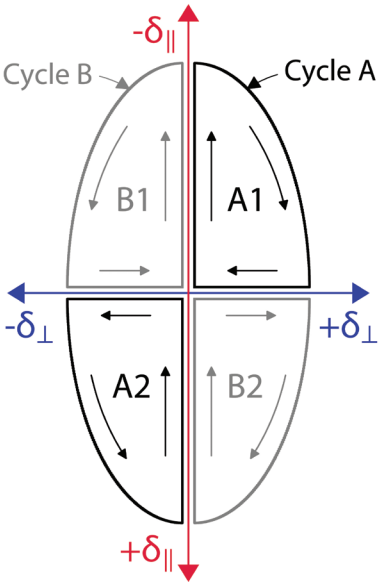

(7d) Test 2 – Elliptical loading pattern with an aspect ratio of 1:0.5

Table 2: Numerical loading sequence of Test 1

Loading Phase	No. of Cycles	Inter-storey drift
Low intensity cycles	2	0.125%
2016 Kaikōura EQ	2	0.25%
	3	0.5%
	5	0.75%
	-	ROM1
	1	1.0%
	1	1.5%
	-	ROM2
Standard Loading Protocol	1	1.5%
	2	2.0%
	2	2.5%
	-	ROM3
	1	3.0%

Table 3: Numerical loading sequence of Test 2

Loading Phase	No. of Cycles	Inter-storey drift
Low intensity cycles	2	0.125%
1994 Northridge EQ	-	-2.0% (‖), +1.0% (‖), +1.0% (⊥), -1.0% (⊥)
	-	ROM1
Standard Loading Protocol	1	1.5%[1]
	1	2.0%[1]
	-	ROM2
	1	2.5%[1]
	1	3.0%[1]
	-	ROM3
	1	3.5%[1]
	1	4.0%[1]
	-	ROM4
	-	+4.0% (⊥),
		-4.0% (⊥),
	1	5.0%[1]

[1] Reflects peak-drift value in (‖) direction. Drift in (⊥) is 50% of the stated (‖) value due to the elliptical loading pattern (Figure 7d).

Because of the quasi-static application of loading, no inertial forces were applied to the specimen and consequently the in-plane diaphragm demands could not be simulated. Nonetheless, to investigate the effect of progressive floor damage on the diaphragm capacity, a deformation pattern referred to as 'rhomboid' loading (ROM) was imposed at different points throughout the earthquake loading phases. The rhomboid loading was applied by horizontally translating the frame at gridline 2 in the positive and negative transverse direction while holding the frame at gridline 1 in place, as schematically shown in Figure 8. For further details on the rhomboid loading, as well as an analysis of the diaphragm performance at different floor damage stages, refer to Parr et al. (2022a; b).

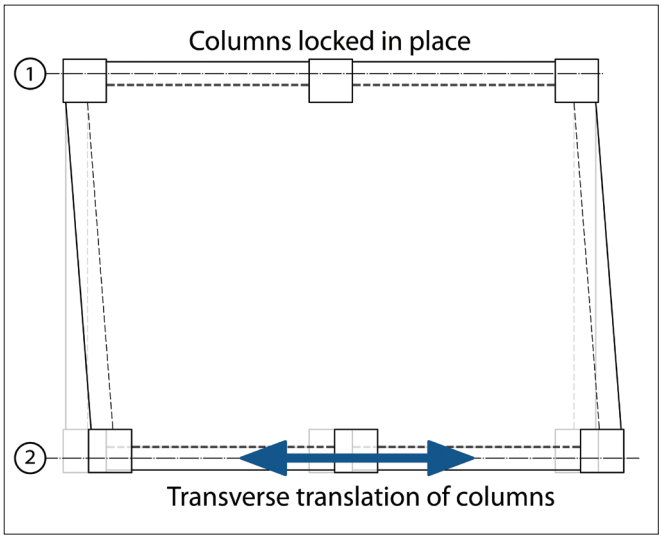

Figure 8: Rhomboid loading

2.4 ASSESSED DRIFT CAPACITY OF THE FLOOR SYSTEM

The drift capacity of the precast floor components in the super-assemblies can be assessed for the three potential failure modes (LOS, NMF and PMF) using the Assessment Guidelines C5 (MBIE et al. 2018). This assessment identifies the drift level at which a flooring unit is expected to lose its reliable gravity load path. This point is unlikely to coincide with the collapse of the flooring unit because precast concrete floors, particularly hollow-core floors, may have unreliable load paths that cannot reliably be quantified and depended on (MBIE et al. 2018).

The assessed drift capacities of the tested flooring units are listed in Table 4. The drift capacities are provided for each failure mode under consideration of the different demands based on the flooring unit's location relative to the parallel beams. All listed drift capacities exclude the factor of 2, which is used in the Assessment Guidelines C5 to account for the uncertainties in estimating the drift demands and capacities and the step-change nature of the floor performance when the demands exceed these capacities. For simplicity, the LOS assessment was conducted assuming a specified seating length of 50 mm and construction tolerances of 20 mm. The assessment of the floor diaphragm is omitted in this paper.

Table 4: Assessed drift capacities based on the Assessment Guidelines C5 (excluding factor 2)

Failure mode	Units affected	Limiting drift
LOS1*	U1,U2,U7,U8	1.2%
LOS2*	All	1.3%
NMF	All**	1.0%
PMF1*	U1,U2,U7,U8	2.0%
PMF2*	All	3.1%
PMF3*	U1,U8	1.4%

Footnote:

* Drift capacities depend on the displacement demands, which are defined as follows:

PMF1 – Demands due to support rotation and elongation of the parallel beam (within elongation zone)

PMF2 – Demands due to support rotation and unit movement due to plastic elongation of the starter bars (outside elongation zone)

PMF3 – Demands due to displacement incompatibility between floor and parallel beam (alpha units only)

** NMF is precluded for the mesh only configuration (U1-U4 at North support of test specimen 2) and where supplemental negative moment reinforcement was installed (U6-U7 of test specimen 1)

3 QUALITATIVE DAMAGE OBSERVATIONS

The qualitative observations of floor damage relative to the imposed inter-storey drift demands are outlined in this section. A more detailed description and forensic analysis of this damage is not addressed in this paper but will form part of a PhD thesis (Büker (In Preparation)).

3.1 FLOOR DAMAGE IN TEST 1

This section outlines the observed floor damage from Test 1 chronologically. The progression of damage in the floor is also summarised in Figure 11, where the key damage states are plotted against the imposed peak drifts. Visualisations of the floor damage in the form of photos and crack maps are presented sequentially in Figure 12.

As described above, the first test simulated the 2016 Kaikōura earthquake followed by a standard loading protocol with progressively increasing inter-storey drifts.

2016 Kaikōura Earthquake (KEQ)

During loading the first sign of floor damage occurred at +0.25% (⊥) inter-storey drift when a longitudinal split (0.4 mm wide) formed between the beta units U4 and

U5 (Figure 12a). This split was initiated by the transverse displacement demands that arise from the rotation and elongation of the beams connecting into the intermediate columns, as schematically demonstrated in Figure 9.

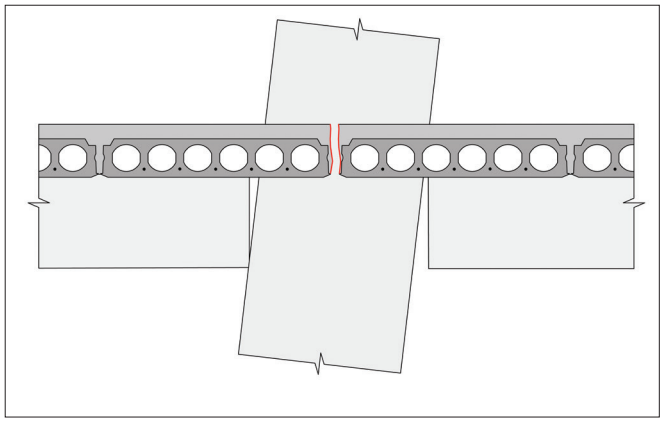

Figure 9: Transverse displacement demands generating split (shown in red) between beta units (deformation exaggerated for clarity)

During the load cycles to 0.5% drift, a substantial amount of new cracking occurred with three main locations of cracking. Firstly, longitudinal splits formed down the first cell of the alpha units U1 and U8 while loading to ±0.5% (⊥) drifts. Secondly, transverse soffit cracks along the seating ledge of the support beams in alpha and beta units occurred when loading to ±0.5% (||) drift. Lastly, the warping deformations due to the simultaneous bi-directional loading generated cracks around the columns in the soffit and top of the floor (refer to Figure 12b).

Although, at this stage, there was only minor cracking visible on the exterior of alpha unit U8, a web crack was suspected of having formed at the south support during the 0.5% drift cycles. This web crack was detected through simple acoustic testing by tapping a hammer on the underside of the floor lengthways along the webs. A distinct difference in the pitch of the sound response could be heard where the crack was suspected. Nonetheless, visual confirmation of the crack was not possible with a borescope camera at this stage. The web crack at this previously identified location became clearly visible at +1.0% (||) drift, as indicated in Figure 12c.

At +1.5% (||) the transverse soffit cracks along the south support of the units had widened substantially. Most notably, the transverse soffit crack in beta unit U4 measured 4 mm with a vertical offset of 2.7 mm and the soffit corner crack in alpha unit U1 measured 3.8 mm in width with a vertical offset of 2.5 mm. These observations are of particular significance because a vertical dislocation in excess of 2 mm is considered an indicator that the reliable gravity load paths between the floor and the support have been lost (Corney et al. 2021).

With further progression of loading, the elongation from the plastic hinges at the intermediate columns B1 and B2 concentrated in the split between the two beta units U4 and U5. As a result, the non-ductile 665 mesh wires across the split fractured while loading to +1.5% (⊥) drift (Figure 12d).

At this point in the test, the beams had sustained extensive cracking in the plastic hinges, resulting in a significant reduction in the torsional stiffness of the damaged beam hinges. Furthermore, dilation of the frame due to beam elongation induced tension in the starter bars which extend from the top of the beam into the floor topping. This eccentrically acting tension force in the starter bars combined with the eccentrically acting floor weight with respect to the centre of the beam caused the beam to sustain a permanent positive rotation relative to the floor. This behaviour had three critical effects on the floor performance:

1. As the beams were no longer fully constrained to twist as drift was imposed on the columns, the relative rotations between the floor and the beams decreased, particularly for the units closer to the midspan of the beam, as indicated in Figure 10.
2. A permanent relative positive rotation between the support beam and the floor meant an increase in seating demands or widening of the positive moment cracks.
3. The behaviour described in above points (1) and (2) also resulted in the relative negative rotations between the floor and the support (remaining small after the beams lost torsional stiffness). Thus, the negative moment demands at the end of the starter bars, which is the critical section for negative moment failure, were relieved to some extent thus decreasing the potential for negative moment failure.

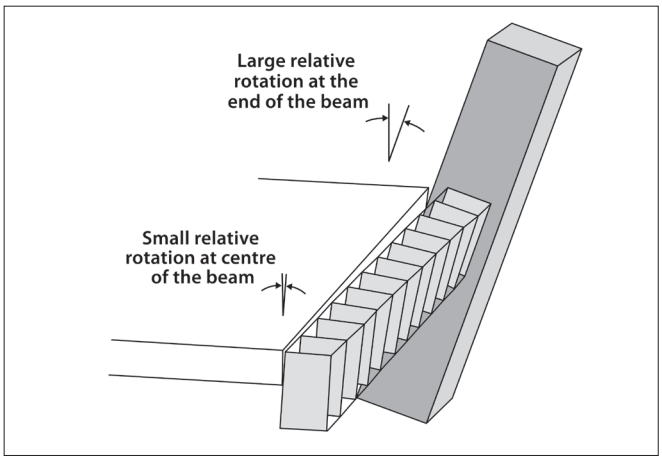

Figure 10: Schematic demonstrating the effect of reduced torsional stiffness in the support beam on the relative rotation between the floor and beam (adapted from Matthews (2003))

Standard Loading Protocol (SLP)

Despite the reduced relative rotation demand on the floor, additional damage was observed during the standard loading protocol phase particularly in locations already damaged during the 2016 Kaikōura earthquake simulation.

Throughout the seismic loading, splitting cracks along the column ties had developed in the vicinity of the intermediate columns. During the cycles to 2.0% and 2.5% the topping concrete over the column ties at the face of the columns spalled off, exposing the reinforcement (Figure 12e).

From the borescope inspections conducted during the 2.5% drift cycles it was concluded that web cracking was present in multiple locations, as indicated in Figure 12f. Only alpha and beta units exhibited web cracking in this first test. The majority of detected web cracks were an extension of the soffit cracks and propagated at an angle of 45° or steeper in the direction of the gravity shear, which is consistent with the positive moment crack propagation observations from Matthews' super-assembly experiment (2003, see Figure 2).

The first experiment was terminated after finishing the 3% drift cycles due to an actuator control error.

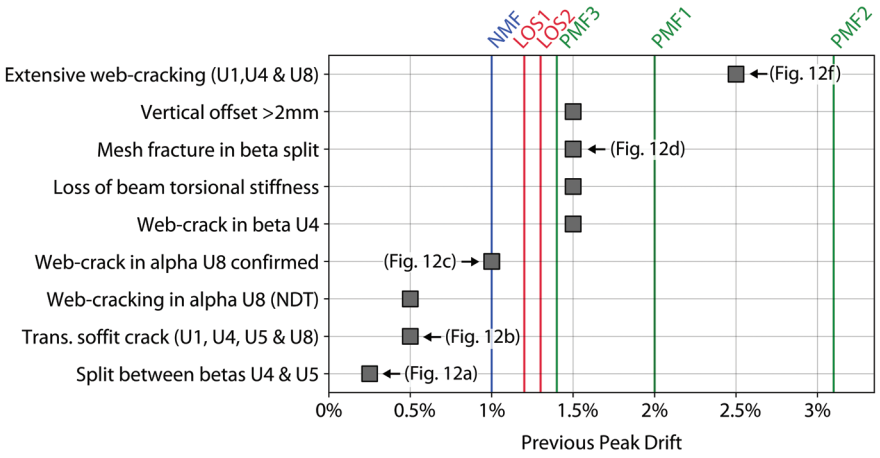

Figure 11: Summary of damage observed in first experiment (refer to Section 2.4 for the definition of failure modes)

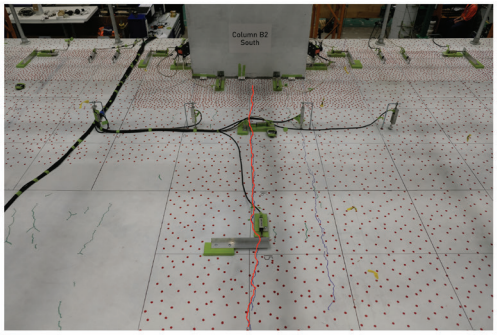

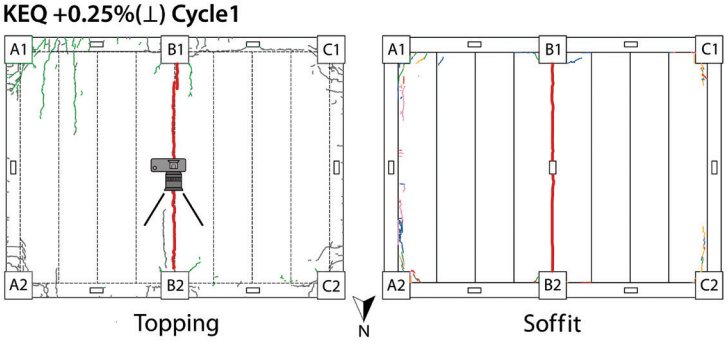

12(a) Full-length longitudinal split between the two beta units shown after 0.25% drift cycles.

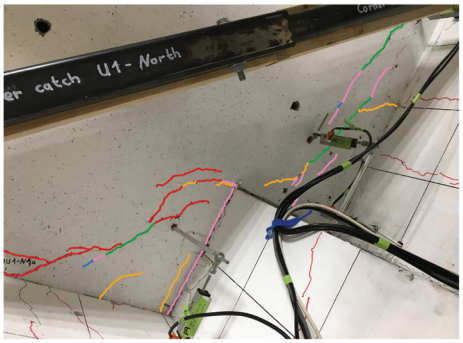

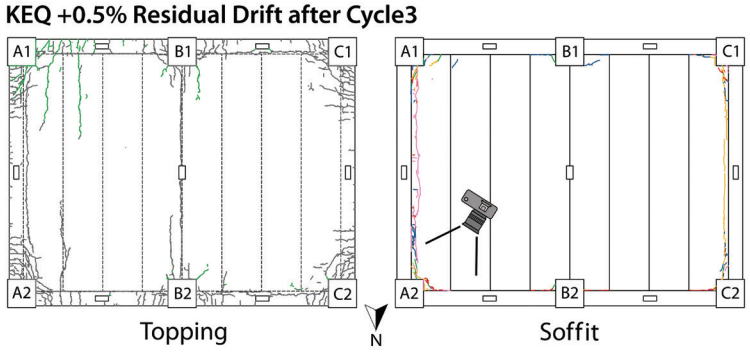

12(b) Transverse soffit cracking in alpha and beta units, longitudinal splits through the first cell of alpha units U1 and U8, and increased cracking around the corners during the 0.5% cycles.

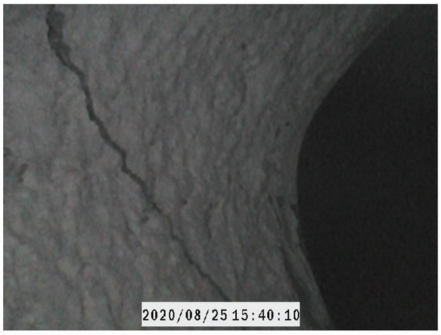

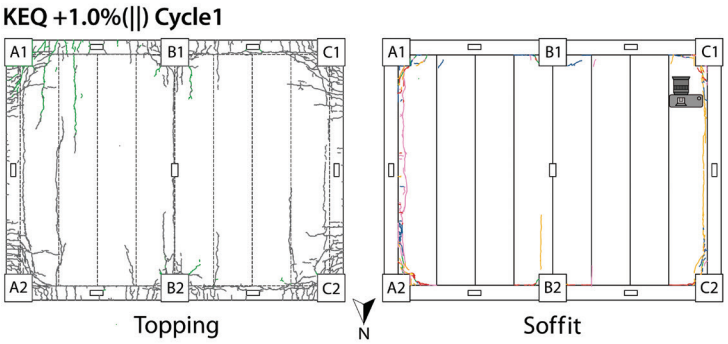

(12c) Web crack in alpha unit U8 at +1.0% (||) (where at 0.5% drift a web crack was detected via acoustic testing)

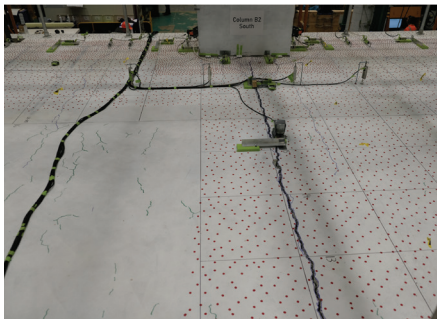

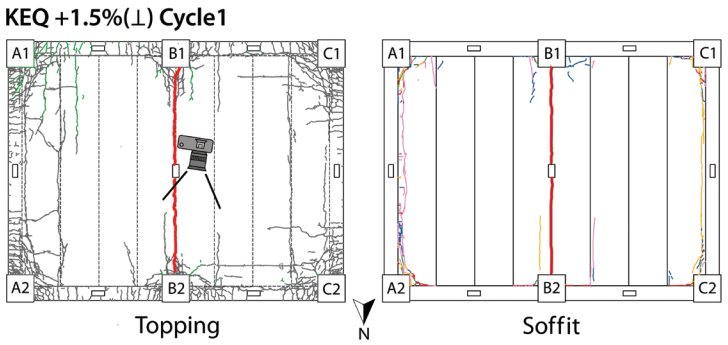

(12d) Widened longitudinal split between beta units after rupture of mesh reinforcement shown after 1.5% drift cycles

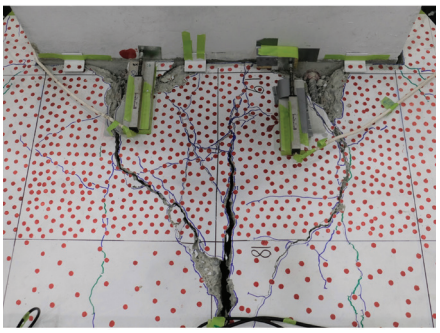

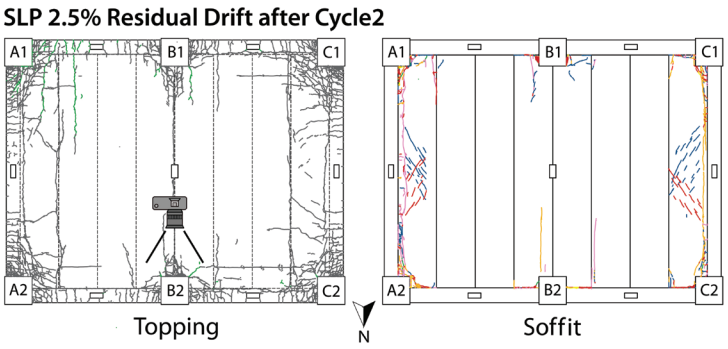

(12e) Extensive spalling and splitting cracks at 2.5%

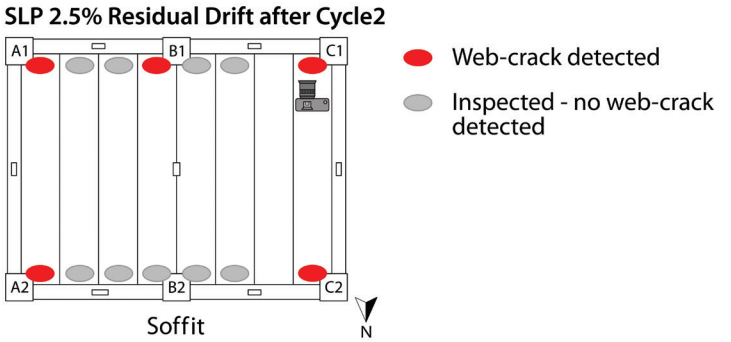

(12f) Extensive web cracking in multiple hollow-core unit ends at 2.5%

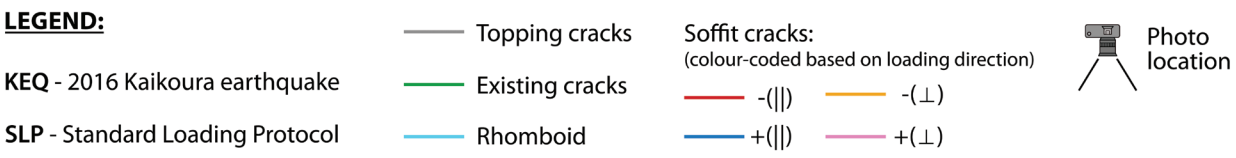

Figure 12: Floor damage observed in Test 1

Gravity test of earthquake damaged hollow-core units

Following the seismic loading, a gravity test was conducted on beta unit U4. The objective of this gravity test was to investigate the residual gravity load-carrying capacity of an earthquake-damaged hollow-core unit. Prior to testing the hollow-core unit of interest was isolated by removing the adjacent flooring units to avoid load sharing between units and allow for a clear view of the sides. The gravity load was applied by placing 1000-litre water tanks on the hollow-core unit and slowly filling the tanks with water.

The actuator control error at the end of the first test mainly affected beta unit U4 at the south support because column B1 was accidentally pulled outwards by 29 mm when the specimen was at -1.5% (||). Before the gravity test the loading error was partially corrected by pushing the column back inwards by 8.3 mm and bringing the specimen into the upright position (0% (||) drift). This correction reinstated the initial conditions to a satisfactory extent because the displacements imposed by the loading error concentrated at the back face of the unit and did not cause noticeable additional damage to the hollow-core unit itself. The web cracking and delamination that beta unit U4 sustained during the earthquake loading are illustrated in Figures 13 a - d. As shown in Figure 13b, the floor was only partially seated.

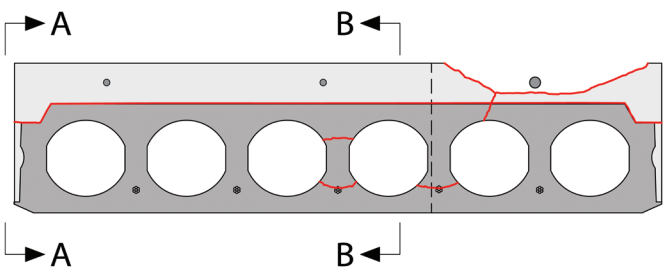

(a) Existing web cracking before the gravity test (Note: This figure only shows the web cracks that were detected by borescope)

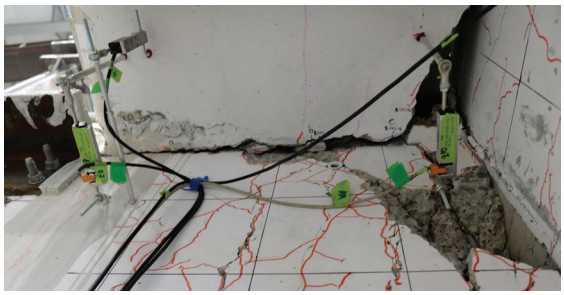

(b) Bottom-view

(c) Side-view from the East (Section A-A in Figure 13a)

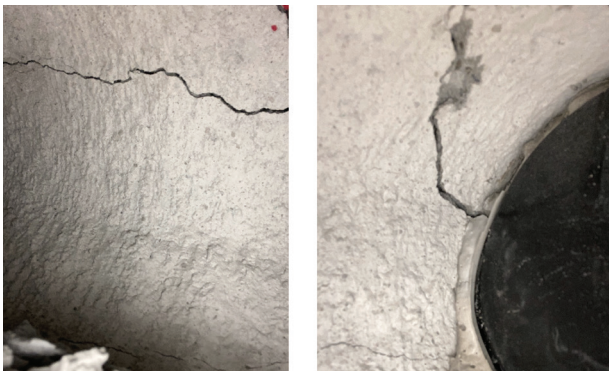

(d) Web cracks in central web (Section B-B in Figure 13a)

Figure 13: Condition of beta unit U4 (south support) after seismic demands and before gravity test

During the gravity test, beta unit U4 could sustain shear loads of up to 38.7 kN and sudden brittle failure occurred when this load was reached, as shown in Figure 14a. Further drop was prevented by the SHS that was installed as a seismic 'catch beam' retrofit underneath this hollow-core unit as part of the overall retrofit solutions (Table 1). Extraction of the failed beta unit U4 gave further insights into the failure mechanism. While the outer web failed in a shallow web-shear crack (Figure 14a), the three interior webs sheared off at a much steeper angle (Figure 14b).

(a) Side-view after failure

(b) Photo of failed end after the extraction

Figure 14: Gravity Test of a damaged beta unit U4.

The shear load of 38.7 kN at which the hollow-core unit failed corresponds to 91% of the design gravity shear demand (1.2G+1.5Q with Q = 3.0 kPa). When comparing the measured shear loads to the design web-shear capacity, they correspond with 52% of the design web shear capacity per NZS3101:2006-A3 (SNZ 2017) when accounting for the reduced section due to the notches and omitting the strength reduction factor of 0.75. While only indicative, given the wide variability in web damage expected in beta units due to earthquake damage and potential effect from the actuator control issue, the test results give a sense of how much web cracking may compromise the residual gravity capacity of hollow-core floors.

The finding that web damage reduces the strength of hollow-core units is consistent with the fact that the shear design of hollow-core floors is done under the presumption that the unreinforced webs remain uncracked. El-Sayed et al. (2019) and Sarkis et al. (2022) conducted experimental component tests on the web-shear cracking behaviour of hollow-core floors, including the post-cracking behaviour. The experiments showed that the load-carrying capacity of the hollow-core units is compromised and reduces substantially once a web-shear crack through the webs has formed. These observations, along with the findings from the gravity test presented in this study, validate concerns regarding how much earthquake-induced damage (in particular, web cracking) compromises the gravity load-carrying capacity of hollow-core units. Further research is required to investigate this matter, given that it was observed in this test that web cracks can form at drifts as low as 0.5% and that many buildings with hollow-core floors in Wellington likely experienced drift demands larger than 0.5% during the 2016 Kaikōura earthquake.

3.2 FLOOR DAMAGE IN TEST 2

The second specimen was loaded with a pulse-type motion from the 1994 Northridge Earthquake, followed by progressively increasing drifts (Figure 7b). The progression of damage is described below and summarised in Figure 15.

1994 Northridge Earthquake (NEQ)

The first pulse to -2.0% (||) drift, as part of the 1994 Northridge earthquake loading, caused extensive damage to the floor. When the pulse reached -0.35% (||) drift, a negative moment crack formed in the saw-cut at the end of the starters along beam B1 C1. The detailing along this support beam (Figure 6b) was intentionally designed to be particularly critical for negative moment failure.

Subsequently the first web cracking was detected at -0.5% (||) drift in units U7 and U8 (North end), as shown in Figure 16a. Although the detected web cracks were an extension of the aforementioned negative moment crack, the low drift at which these web cracks formed highlighted the fragility of the unreinforced webs. The detection of such narrow web cracks with a borescope camera was difficult due to the challenging navigation of the borescopes and poor lighting conditions in the voids. Furthermore there was no indication of the web crack through damage on the underside of the floor because the web crack was an extension of the negative moment cracking that initiated at the top of the floor.

The first transverse soffit cracking occurred along the north support at -0.5% (||) and additional soffit cracks formed while loading to -0.75% (||) drift. Most notably a transverse soffit crack formed 200-350 mm away from the support in alpha unit U1 (Figure 16b). Although the soffit crack only measured 0.3 mm in width, it propagated internally as a diagonal web crack in the direction of the gravity shear towards the top of the unit. This soffit crack had initiated at

the corner of the notch that was cut into the unit to fit the alpha unit around the precast columns. Thereby, this crack demonstrated how the notches acted as a stress raiser that promoted soffit and web cracking away from the support. Similarly the presence of the stitching bars that were installed transversely along the column ties acted as a stress raiser, promoting a negative moment crack near the end of the starter bars along support A1-B1 (see topping crack map in Figure 16b).

At -1.0% (||) drift a vertical offset of 1.3 mm across the soffit crack at the north support of beta unit U5 was measured. During the loading to -1.5% (||) drift the vertical offset across the now 3 mm wide soffit crack increased to 2.6 mm and thus exceeded the vertical offset benchmark of 2 mm, which indicates a loss of reliable load path (Corney et al. 2021). The vertical offset measured across the soffit crack in beta unit U4 (north end) was even more pronounced, measuring 3.7 mm. This soffit crack formed approximately 100 mm from the support beam ledge and propagated internally as a shallow web crack approximately 400-500 mm towards mid-span, as shown in Figure 16c.

With further loading the negative moment crack at the end of the starter bars along beam B1-C1 continued to widen. From -1.6% (||) onwards, the 665 mesh at the end of the starter bars fractured starting at column C1 and progressing to column B1. When -2.0% (||) drift was reached the width of the negative moment crack ranged from 3.5 mm (at beta unit U5 – Figure 16d) to 5.0 mm (at alpha unit U8) and a substantial vertical offset of up to 3.2 mm (at beta unit U5) was measured across this crack.

The presence of web cracking in every hollow-core unit was confirmed at the peak of the first pulse (-2.0% (||) drift) as indicated in Figure 16e. Furthermore additional vertical offsets across the transverse cracks in the soffit of beta units U4 and U5 were recorded, with a magnitude of 6 mm and 4.5 mm respectively. Figure 16f illustrates the extent of the vertical offset in beta unit U5. It should be noted that further vertical offset of beta unit U5 was prevented by the strongback retrofits, but the cable-catch retrofit under beta unit U4 allowed for additional vertical offset.

During drift demands in the transverse direction (±1.0% (⊥)) it became evident that the stitching bars (see Figure 6b) prevented the formation of a single dominating longitudinal split between the beta units as was previously observed in the first test. Instead the transverse deformation demands distributed to several longitudinal splits that had predominantly formed beyond the stitching bars.

Standard Loading Protocol (SLP)

Further significant damage to the hollow-core floor was observed during the standard loading protocol phase (Figure 7b). At +1.6% (||) drift the mesh at the floor perimeter along beam A2-B2 fractured during loading to +2.0% (||) drift. This particular support comprised no starter bars but only 665 mesh that extended from the topping into the top of the beam. Following the fracture of the mesh, the previously distributed negative moment cracking in the floor topping closed up and deformations started to concentrate in the crack where the mesh ruptured, subsequently behaving as a pinned support.

With increased peak displacements the web cracks widened substantially, as demonstrated by the borescope photo depicted in Figure 16g at -2.5% (||) drift. Despite the significant width of web cracks at peak drift the web cracks were found to close up when the test specimen was moved to residual displacement. This observation has two key implications for a post-earthquake inspection. Firstly, the inspection for web cracks in real buildings can be challenging with the web cracks having closed. Secondly, the width of the web crack after the earthquake cannot directly be correlated to the length and extent of the web crack.

With the progression of loading the gravity load paths at the end supports of the flooring units became heavily compromised. The strongback retrofits that were installed under units U5-U8 successfully limited the vertical offset, whereas the cable-catch retrofits that were installed under units U1-U4 required the floor to drop before the cables engaged. During the 3% drift cycles units U3 and U4 had sustained a large vertical offset while units U1 and U2 experienced comparatively little vertical offset. This limited offset could be attributed to load sharing between the parallel beam A1-A2, unit U1 and unit U2. Although this load path is structurally unreliable it evidently helped prevent the units from sustaining excessive vertical drop at this stage of the test.

During loading to 3.5% (||) drift the mesh along beam A1 B1 fractured in a negative moment crack at the end of the starter bars. This negative moment crack propagated from the stitching bars across the units U1-U4 and merged with a flexural crack in the top of the beam A1-A2. At this support the starter bar configuration was assessed to be on the verge of being prone to negative moment failure using the Assessment Guidelines C5 (MBIE et al. 2018). A possible interpretation is that the yield force of the starter bars acting in tension was not sufficient to fracture the mesh at the end of the starter bars, but the strain hardening of the starter bars was sufficient to trigger the negative moment failure. Following this failure the floor sustained a

significant vertical displacement, leading to all hollow-core floor units being at least partially supported by the retrofits.

During the fourth rhomboid (ROM4) the northern frame was displaced transversely by +34 mm and -32 mm. At +34 mm transverse displacement the mesh along the west end of the stitching bars fractured, resulting in a wide longitudinal split running through beta unit U5 (Figure 16h).

At -4.0% (⊥) drift a secondary crack in the bottom part of beta unit U4 along the edge of the seating angle formed when the floor engaged with the angle, which was intentionally set down by 40 mm (Figure 16i). The collapse of the hollow-core unit was prevented by the cable-catch system that was anchored back to the seating angle. Nonetheless, this crack highlights the fragility of hollow-core units that have sustained shallow web cracking and indicates that seating angle retrofits may not be suitable solutions to address this damage (Brooke et al. 2022; SESOC et al. 2021).

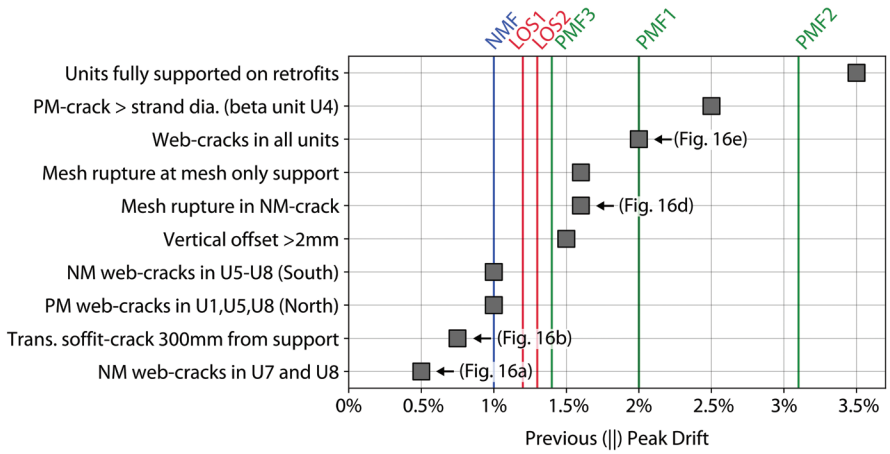

Figure 15: Summary of damage progression of Test 2 (refer to Section 2.4 for the definition of failure modes)

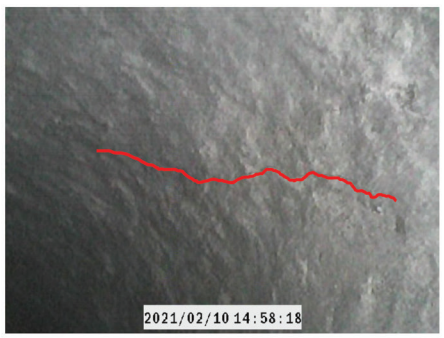

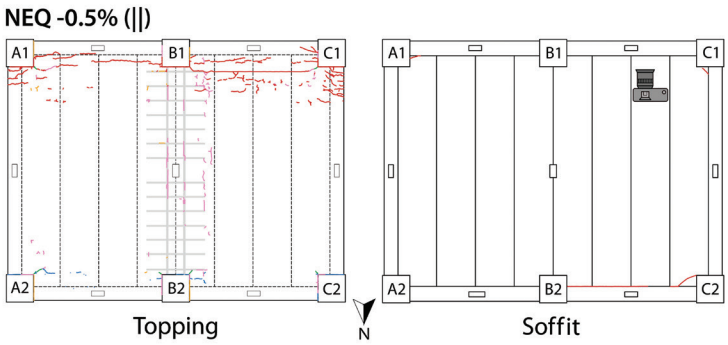

(a) First web crack in Unit U7 (illustrated in the photo) and alpha unit U8 – crack is highlighted in red

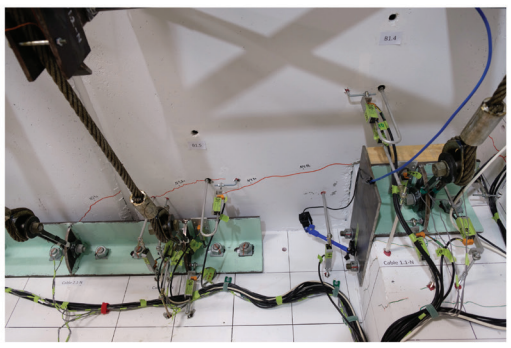

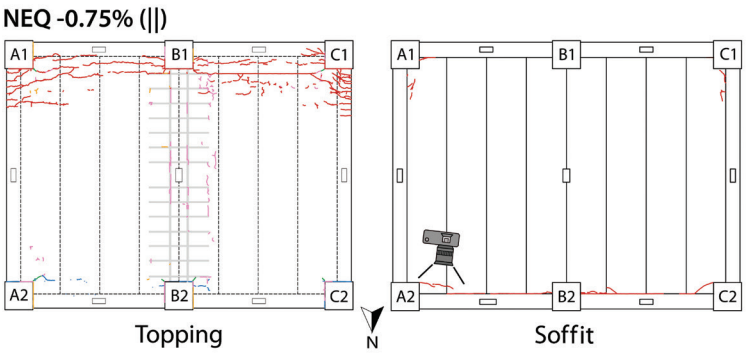

(b) Transverse soffit crack approx. 200-350 mm away from the support ledge (Alpha U1 – North)

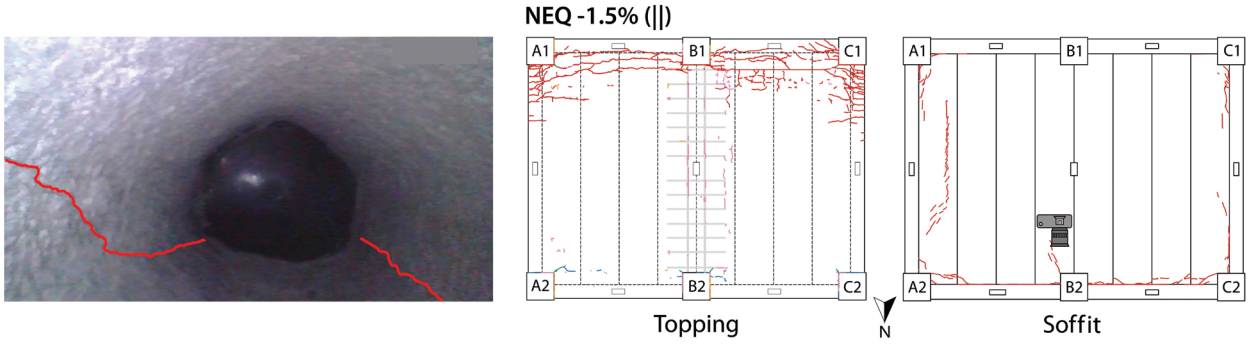

(c) Web cracking in beta unit U4 (North support)

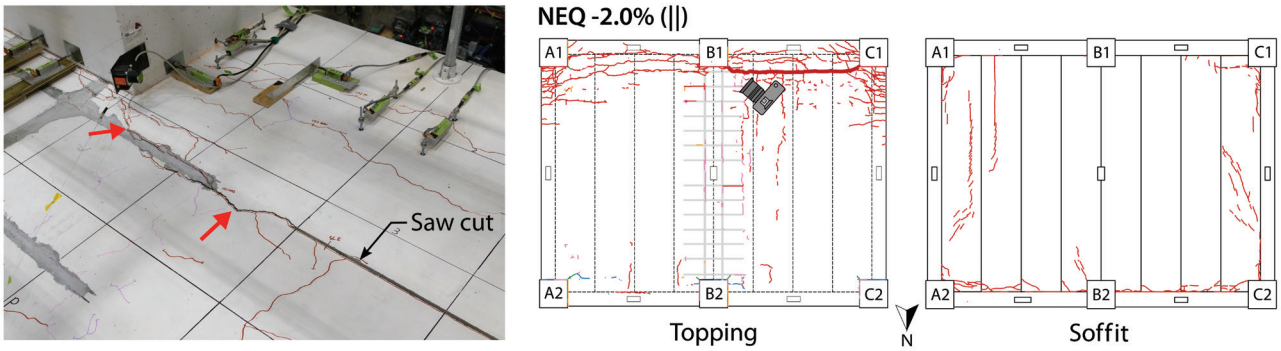

(d) Negative moment crack shown at -2.0% (||) after mesh rupture at -1.6% (||)

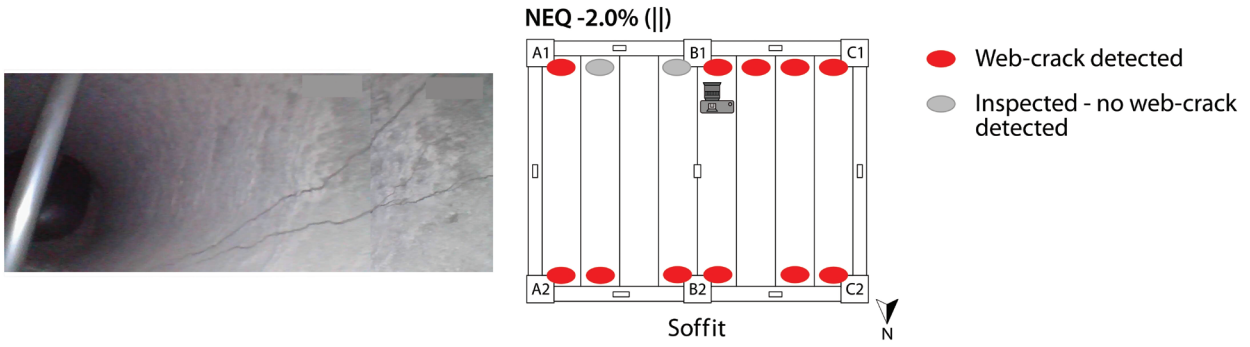

(e) Web cracking at -2.0% (||). The photo shows a web crack that is an extension of the negative moment crack in unit U5.

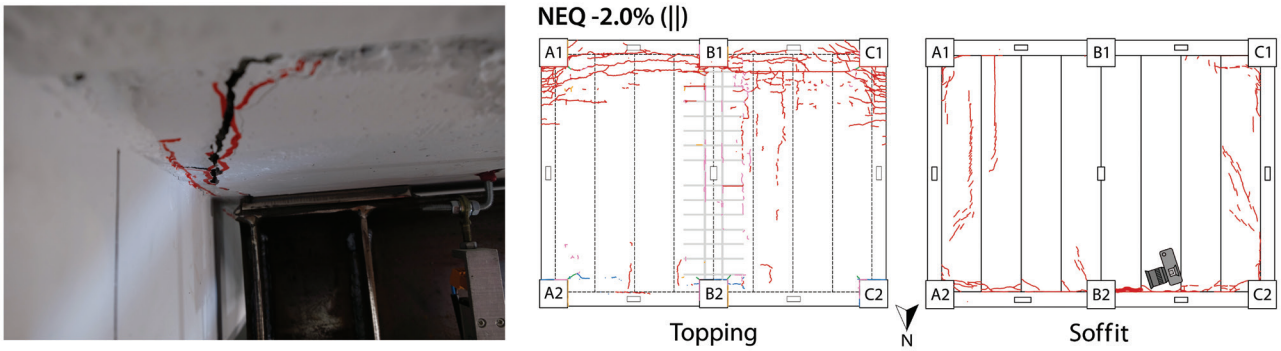

(f) Vertical offset in beta unit at -2.0% (||)

(g) Shallow diagonal web crack in unit 2 at -2.5% (||)

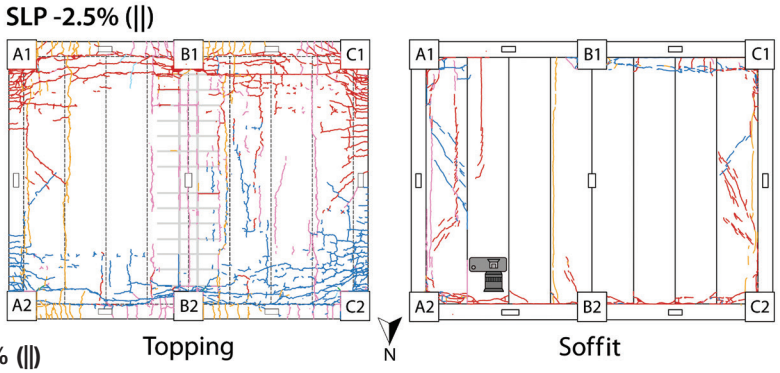

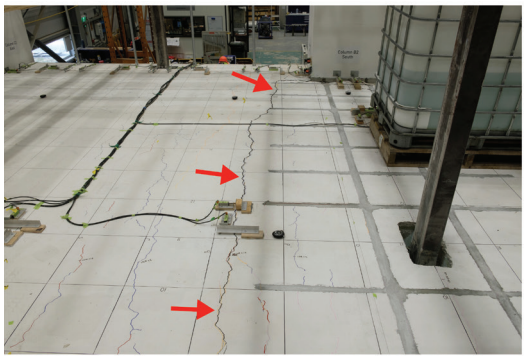

(h) Mesh rupture in a longitudinal split running through the last cell of beta unit U5

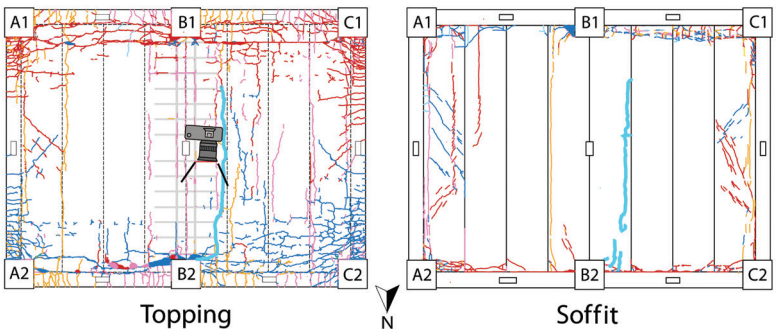

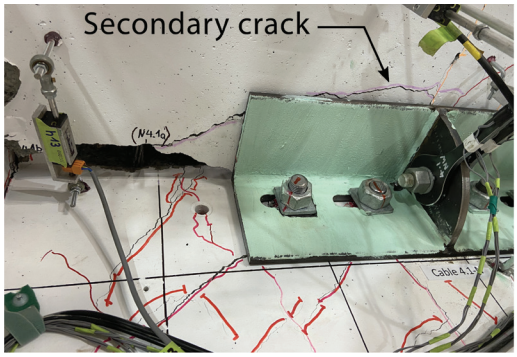

i) Secondary cracking in the bottom flange of unit formed when floor drops on set-down angle.

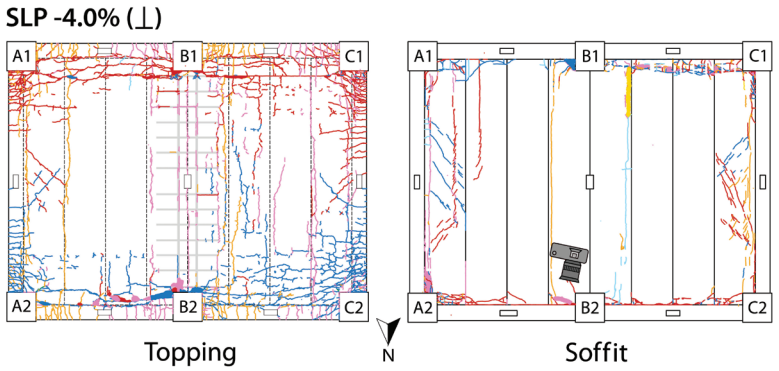

LEGEND:

NEQ - 1994 Northridge earthquake

SLP - Standard Loading Protocol

Existing cracks

Rhomboid

Topping and soffit cracks:
(colour-coded based on loading direction)

-(||)

-(⊥)

+(||)

+(⊥)

Photo location

Figure 16: Floor damage observed in Test 2

3.3 COMPARISON OF FLOOR DAMAGE PROGRESSION OF TESTS 1 AND 2

When comparing the extent of floor damage observed in the two super-assembly tests, it can be summarised that the second test exhibited more severe damage to the floor than the first test. The difference in damage levels can primarily be attributed to the early loss of torsional stiffness in the supporting beams during the first test. As described in Section 3.1 the loss of torsional stiffness in the beams decreases the relative rotation between the floor and the beam which leads to a reduction in demands and, consequently, less damage to the floor. This effect has also been observed in previous super-assembly tests (Lindsay 2004; MacPherson 2005; Matthews 2003; Peng 2009).

A further contributing factor to the limited amount of floor damage in the first test was the softening of the floor perimeter through a large number of cycles at relatively low inter-storey drifts (e.g. 1% drift) in the 2016 Kaikōura earthquake input motion. With the softened perimeter, additional deformations concentrated in the damage at the floor-to-beam interface in the first test. This observation contrasts with the damage observed in the second test, where the pulse-type nature of the 1994 Northridge earthquake with the initial monotonic pulses to -2% (||) and +1% (||) in the direction of the floor span caused significantly more transverse cracking and associated web cracking within the hollow-core units.

In addition, the shallow nature of the web cracks and the presence of soffit cracks forming away from the support observed in the second test stood out. These damage patterns draw into question the efficacy of seating retrofits, such as seating angles, to address positive moment failures. (Brooke et al. 2022; Büker et al. 2021; SESOC et al. 2021).

In both tests beta units were found to sustain a higher degree of damage than units seated outside the plastic hinge region. This statement is based on test observations indicating a concentration of damage in beta units with (1) earlier onset of web cracking, (2) more extensive web cracking, (3) larger vertical offsets and (4) susceptibility to large longitudinal splits. Mostafa et al. (2022) further elaborate on the vulnerabilities of beta units and emphasise that the damageability of these units is neither considered in the current New Zealand Concrete Structures Standard NZS3101:2006-A3 (SNZ 2017) nor in the Assessment Guidelines C5 (MBIE et al. 2018).

These two super-assembly tests also showed that the detailing of the column ties can have an influence on the location of cracking. In the first test the transverse displacement demands on the floor that arise from rotation and elongation of the beams at the intermediate column (Figure 9) caused a longitudinal split between the two beta units. With the mesh rupturing during the 1.5% drift cycle the floor diaphragm completely separated in this location. For the second test ductile D12 stitching bars were installed transversely across the interface between the beta units U4 and U5 to reinstate the load path across the portion of the mesh that needed to be cut during post-installation of the column ties (Figure 6b). The presence of these stitching bars resulted in the displacements manifesting in a split that formed beyond the stitching bars and through beta unit U5, as shown in Figure 16h. While the stitching bars successfully prevented significant longitudinal splitting along the column ties where the mesh was cut, the splitting shifted beyond the stitching bars, where there was only mesh reinforcing the topping layer (Figure 16h). These observations emphasise the brittleness of floor diaphragms reinforced with non-ductile mesh reinforcement (665 mesh in this case). As a consequence of mesh rupture in these splits, the ability for tension ties to develop as part of the diaphragm strut-and-tie load path is removed, which is further discussed in the companion papers by Parr et al. (2022a; b).

3.4 COMPARISON OF FLOOR PERFORMANCE TO ASSESSED CAPACITY

The seismic assessment of the flooring units (Section 2.4) can be compared to the floor damage observed in the super-assembly tests. Generally, the floor damage in the two experiments was highly variable and it was found that the observed failure pattern does not necessarily reflect the predicted governing failure mode based on the assessment (i.e. failure mode with the lowest assessed drift capacity). For instance, in the second test much of the deformation along the north support between columns A2 and B2 concentrated at the positive moment soffit cracks, while a LOS failure was expected to be the governing failure mechanism as per assessment. This finding underlines the importance of installing floor retrofits that address all failure modes (not only the governing failure mode) with drift capacities lower than the expected demand.

Although the actual failure mechanism sometimes differed from the predicted governing failure mechanism, the assessed drift capacities gave a good indication as to when the floor would lose the reliable load path. Similar to previous work (Corney et al. 2021) the load path of the floor was considered to be unreliable once a vertical drop of 2 mm was reached. In both tests this vertical drop benchmark was exceeded when the peak drifts were increased from 1.0% to 1.5%. These drift levels lie in the range of the typical drift limits for LOS and NMF, as illustrated in the damage summary plots (Figure 11 for Test 1 and Figure 15 for Test 2).

3.5 DETECTION OF WEB CRACKING

Precast hollow-core floors in New Zealand have no vertical shear reinforcement and, thus, rely solely on the capacity of the prestressed concrete to resist shear demands. The shear stresses are highest in the hollow-core floor webs, which are optimised to resist the shear stresses as an uncracked section. However the observed damage from the super-assembly tests shows that the earthquake-induced deformations can result in various degrees of web cracking, initiating at drift levels as low as 0.5%. Web cracks may reduce the gravity load-carrying capacity for both gravity loading and future earthquake loading, as indicated by the results of the gravity test described in Section 3.1. Nonetheless further research is required to reliably quantify the residual gravity load capacity of web-cracked hollow-core units.

Based on the experience gained from the many web crack inspections performed during the super-assembly tests, the following recommendations can be made:

- Web crack inspections should commence on floors/levels which likely experienced the largest interstorey drift in a previous earthquake(s). Additionally, the Assessment Guidelines C5 (MBIE et al. 2018 - Section C5E.2) provide recommendations on where to conduct inspections for precast concrete floors.
- Alpha and beta units are particularly (but not exclusively) vulnerable to web cracking and should be prioritised when conducting an inspection for web cracks.
- Significant cracking in the topping at the end of the starter bars may indicate a negative moment failure, which involves shallow web cracking. Negative moment failure cracks typically run vertically through the topping and top flange of the hollow-core unit but then propagate as shallow web cracks, branching towards the support and usually also towards mid-span. This type of cracking can lead to a sudden collapse even when the mesh is still intact (see Woods (2008) for background information on negative moment failure in hollow-core floors).
- Transverse and diagonal soffit cracks that cross underneath one or multiple webs of the hollow-core unit likely have propagated into the above webs. If there is a vertical offset across the soffit crack, this offset likely reflects the width of the web crack.
- While web cracking associated with positive moment cracking is typically accompanied by soffit cracking, this soffit cracking may not be visible as it may occur behind the support ledge or can be covered by existing retrofits. Beta units can experience web cracks that initiate at the end of the unit. Hence some units without visible soffit or topping cracks may still have experienced web cracking and thus should not be ignored in an inspection protocol.
- When inspecting the interior of a hollow-core unit it is recommended to actively check for potential web cracking during the inspection. Trying to identify web cracks after the inspection from recorded photos and videos is challenging and may require additional inspections to confirm the presence and location of a web crack.
- Web cracks will be challenging to identify after an earthquake when the building has returned to plumb as the cracks will have closed. Not identifying web cracks in the inspection does not necessarily guarantee there are no web cracks present.
- Acoustic testing, such as hammer tapping or more sophisticated non-destructive testing methods, may be helpful to identify web cracks.

4 SUMMARY

This paper presents the progression of hollow-core floor damage from two super-assembly tests. The tested hollow-core floors were constructed using common floor details in New Zealand during the 1980s. The most relevant floor damage observations are as follows:

- Cracking in the unreinforced webs of the hollow-core units initiated at 0.5% drift in both tests. Based on this early onset it may be concluded that many existing hollow-core floor buildings in Wellington that were affected by the 2016 Kaikōura Earthquake and were subjected to drifts equal to or exceeding 0.5% drift contain hollow-core units with cracked webs.
- The detection of the early narrow web cracks in the test specimens was difficult due to poor light conditions and navigation challenges with the borescope camera, even in ideal laboratory conditions. Additionally, web cracks that were of substantial width and length at peak drifts tended to close up at residual displacement. Therefore, inspecting units for web cracks and not identifying any cracks during the inspection does not guarantee that none exist in a building that has experienced drift demands beyond 0.5%. Recommendations are presented on how to identify the hollow-core units that likely sustained web cracks and how to effectively inspect the interior of those flooring units.
- Earthquake damage, particularly web cracking near the support, can decrease the gravity load-carrying capacity of hollow-core floors, as demonstrated by loading an earthquake-damaged unit with gravity weights. The damaged unit only withstood 91% of the gravity design load (1.2G+1.5Q) and 52% of the design capacity according to NZS3101:2006-A3 (SNZ 2017), excluding the strength reduction factor.

- Transverse soffit cracking can occur away from the support and beyond the typical seating retrofits (i.e. seating angles). Hollow-core units with notches are particularly prone to such cracking because the notches act as a stress raiser. Furthermore the web cracks extending from the transverse soffit cracks were found in these tests to propagate at very shallow angles. These findings raise concerns about the ability of seating retrofits to address positive moment failure (Brooke et al. 2022; SESOC et al. 2021).
- Pulse-type ground motions tend to cause more severe damage to the hollow-core floors than far-field ground motions, which involve many smaller cycles leading up to the peak response.
- Hollow-core units seated at the intermediate columns (beta units) are more susceptible to damage than units that are supported closer to the mid-span of the support beam. Whilst alpha units are addressed, the heightened fragility of these beta units is not recognised in the current seismic assessment procedures in the Assessment Guidelines C5 (MBIE et al. 2018) and requires further research.
- The Assessment Guidelines C5 (MBIE et al. 2018) have been found to provide a good indication of the drift capacity of the tested hollow-core floors. However in many instances the observed damage patterns did not reflect the predicted governing failure modes.

5 ACKNOWLEDGEMENT

The authors would like to thank the funders who made the super-assembly tests described in this paper possible. The main funders were BRANZ (from the Building Research Levy), QuakeCoRE, the Earthquake Commission (EQC), Concrete NZ and the University of Canterbury. Blacks Fasteners, Fischer and Hilti kindly sponsored the material for fasteners. Thanks are also extended to the Advisory Group of the 'ReCast Floors' project for the valuable input for developing the tests. The successful delivery of the experimental programme would not have been possible without the countless hours and valuable advice of the technical staff at the University of Canterbury, most notably Dave Carney, Alan Thirlwell, Russell McConchie, Norman King, Dave MacPherson and John Maley. Also noteworthy is the contribution of the many students who helped with the test, namely Eldhose Paulose, Max Chirapattanakorn, Trevor Garrett, Abhishek Madan, Yuxin Huang, Claire Dong, Mohamed Mostafa, Ana Sarkis, Justin Brown, Jacob Nicholls and Alex Kirby.

This project was (partially) supported by QuakeCoRE, a New Zealand Tertiary Education Commission-funded Centre. This is QuakeCoRE publication number 0749.

6 REFERENCES

Brooke, N. J., Büker, F., Bull, D. K., Elwood, K. J., Henry, R. S. and Hogan, L. S. 2022. "Overview of Retrofit Requirements and Techniques for Precast Concrete Floors." Journal of the Structural Engineering Society New Zealand, 35 (1).

Büker, F. (In Preparation). "Development and Experimental Validation of Hollow-core Floor Retrofits." PhD Thesis. University of Auckland, New Zealand.

Büker, F., Brooke, N. J., Elwood, K. J., Bull, D. K., Hogan, L. S. and Parr, M. 2021. "Development and Validation of Retrofit Techniques for Hollow-core Floors." Proceedings of the 2021 SESOC Conference, 14. Hamilton, New Zealand: Structural Engineering Society New Zealand.

Büker, F., Brooke, N. J., Hogan, L. S., Elwood, K. J., Bull, D. K. and Sullivan, T. J. 2022. "Design Recommendations for Strongback Retrofits." Journal of the Structural Engineering Society New Zealand, 35 (1).

Bull, D. K., and Matthews, J. 2003. Proof of Concept Tests for Hollowcore Floor Unit Connections (Research Report 2003-1). 1–84. Department of Civil Engineering, University of Canterbury.

Chandramohan, R., Ma, Q., Wotherspoon, L. M., Bradley, B. A., Nayyerloo, M., Uma, S. R. and Stephens, M. T. 2017. "Response of instrumented Buildings Under the 2016 Kaikoura Earthquake." BNZSEE, 50 (2): 237–252. https://doi.org/10.5459/bnzsee.50.2.237-252.

Corney, S. R., Elwood, K. J., Henry, R. S. and Nims, D. K. 2018. Assessment of Existing Concrete Buildings in Wellington with Precast Floors. Kaikoura Earthquake Research Programme (2017-18). Lower Hutt, New Zealand: Natural Hazards Research Platform.

Corney, S. R., Puranam, A. Y., Elwood, K. J., Henry, R. S. and Bull, D. K. 2021. "Seismic Performance of Precast Hollow-Core Floors: Part 1—Experimental Data." ACI Structural Journal, 118 (5): 49–64. https://doi.org/10.14359/51732821.

De Francesco, G., Sullivan,T. J. and Nievas, C. I. 2022. "Highlighting the Need for Multiple Loading Protocols in Bi-Directional Testing (In Production)." Bulletin of the New Zealand Society for Earthquake Engineering, 15.

El-Sayed, A. K., Al-Negheimish, A. I. and Brennan, A. M. 2019. "Web Shear Resistance of Prestressed Precast Deep Hollow Core Slabs." ACI Structural Journal, 116 (1): 139–150. https://doi.org/10.14359/51706919.

Fenwick, R., Bull, D. K., and Gardiner, D. 2010. Assessment of Hollow-Core Floors for Seismic Performance (Research Report 2010-02). University of Canterbury, Christchurch, New Zealand (https://ir.canterbury.ac.nz/handle/10092/4211).

Henry, R. S., D. Dizhur, K. J. Elwood, J. Hare, and D. Brunsdon. 2017. “Damage to Concrete Buildings with Precast Floors During the 2016 Kaikoura earthquake.” Bulletin of the New Zealand Society for Earthquake Engineering, 50 (2): 174–186.

Herlihy, M. D. 1999. “Precast Concrete Floor Support and Diaphragm Action.” PhD Thesis. University of Canterbury, Christchurch, New Zealand.

Jensen, J. 2006. “The Seismic Behaviour of Existing Hollowcore Seating Connections Pre and Post Retrofitted.” ME Thesis. University of Canterbury, Christchurch, New Zealand.

Liew, H. Y. 2004. “Performance of Hollow-core Floor Seating Connection Details.” ME Thesis. University of Canterbury, Christchurch, New Zealand.

Lindsay, R. 2004. “Experiments on the Seismic Performance of Hollow-core Floor Systems in Precast Concrete Buildings.” ME Thesis. University of Canterbury, Christchurch, New Zealand.

MacPherson, C. 2005. “Seismic Performance and Forensic Analysis of a Precast Concrete Hollow-Core Floor Super-Assemblage.” ME Thesis. University of Canterbury, Christchurch, New Zealand.

Matthews, J. 2003. “Hollowcore Floor Slab Performance Following a Severe Earthquake.” PhD Thesis. University of Canterbury, Christchurch, New Zealand.

MBIE, EQC, NZSEE, SESOC, and NZGS. 2018. Technical Proposal to Revise the Engineering Assessment Guidelines - Part C5 Concrete Buildings. Wellington, New Zealand: Ministry of Business, Innovation, and Employment.

Mejia-McMaster, J. C. 1994. “Precast Concrete Hollow-core Floor Unit Support and Continuity.” ME Thesis. University of Canterbury, Christchurch, New Zealand.

Mostafa, M. T., Büker, F., Hogan, L. S., Elwood, K. J., Bull, D. K. and Parr, M. 2022. “Seismic Performance of Precast Hollow-core Units Seated Within the Plastic Hinge Region.” Proceedings of the 2022 NZSEE Annual Technical Conference, 12. Wellington, New Zealand: New Zealand Society for Earthquake Engineering.

Norton, J. A., King, A. B., Bull, D. K., Chapman, H. E., McVerry, G. H., Larkin, T. J. and Spring, K. C. . 1994. “Northridge Earthquake Reconnaissance Report.” Bulletin of the New Zealand National Society for Earthquake Engineering, 27 (4): 235–344. Bulletin of the New Zealand National Society for Earthquake Engineering, December, Vol. 27, No.4.

Oliver, S. J. 1998. “The Performance of Concrete Topped Precast Hollowcore Flooring Systems Reinforced with and Without Dramix Steel Fibres Under Simulated Seismic Loading.” ME Thesis. University of Canterbury, Christchurch, New Zealand.

Parr, M., Büker, F., De Francesco, G., Bull, D. K., Brooke, N. J., Elwood, K. J., Hogan, L. S., Liu, A. and Sullivan, T. J. 2022a. “Load-Path and Stiffness Degradation of Floor Diaphragms in Reinforced Concrete Buildings Subjected to Lateral Loading - Part I, Experimental Observations.” Journal of the Structural Engineering Society New Zealand, 35 (1).

Parr, M., Bull, D. K., Brooke, N. J., De Francesco, G., Elwood, K. J., Hogan, L. S., Liu, A. and Sullivan. 2022b. “Load-Path and Stiffness Degradation of Floor Diaphragms in Reinforced Concrete Buildings Subjected to Lateral Loading - Part II, Data Analysis.” Journal of the Structural Engineering Society New Zealand, 35 (1).

PCFOG. 2009. Seismic Performance of Hollow Core Floor Systems - Guidelines for Design Assessment and Retrofit (Preliminary Draft). Precast Concrete Floors Overview Group (SESOC, NZSEE, and NZCS), Wellington, New Zealand. http://www.nzsee.org.nz/db/PUBS/HollowCoreFloorSystems.pdf.

Peng, B. H. 2009. “Seismic Performance Assessment of Reinforced Concrete Buildings with Precast Concrete Floor Systems.” PhD Thesis. University of Canterbury, Christchurch, New Zealand.

Sarkis, A. I., Büker, F., Sullivan, T., Elwood, K. J., Brunesi, E. and Hogan, L. 2022. “Aspects Affecting the Nonlinear Behaviour of Precast Pre-stressed Hollow-core Units Failing in Shear (Accepted and in Production).” Structural Concrete. https://doi.org/10.1002/suco.202100579.

SESOC, NZSEE, and ENZ. 2021. “Advice on Hollow-core Floors.” Accessed October 6, 2021. https://www.sesoc.org.nz/precast-flooring-resources/.

SNZ. 2004. Amendment 3 to the Concrete Structures Standard. NZS 3101:1995-A3. Wellington, New Zealand: SNZ.

SNZ. 2011. Structural Design Actions. Part 0: General Principles (Incorporating Amendments Nos 1,2,3,4 and 5). NZS1170.0:2002. Wellington, New Zealand: SNZ.

SNZ. 2017. Concrete Structures Standard (Incorporating Amendment No. 1,2 and 3). NZS 3101:2006. Wellington, New Zealand: SNZ.

Trowsdale, J. 2004. “Seismic Performance of Hollowcore Seating Detail Specified by Amendment No 3 NZS 3101:1995.” Bachelors (Honours) - Final year project report. University of Canterbury, Christchurch, New Zealand.

Woods, L. J. 2008. “The Significance of Negative Bending Moments in the Seismic Performance of Hollow-Core Flooring.” ME Thesis. University of Canterbury, Christchurch, New Zealand, 294p.

ISSN No. 2744-7871